UNIVERSITÀ DEGLI STUDI DI BERGAMO
DIPARTIMENTO DI INGEGNERIA DELL'INFORMAZIONE
E METODI MATEMATICI°

QUADERNI DEL DIPARTIMENTO

Department of Information Technology and Mathematical Methods

Working Paper

Series "*Mathematics and Statistics*"

n. 8/MS – 2009

Comparative finite-element model analysis of ascending aortic flow in bicuspid and tricuspid aortic valve

by

**F. Viscardi, C. Vergara, L. Antiga, S. Merelli, A. Veneziani,
G. Puppini, G. Faggian, A. Mazzucco, G.B. Luciani**

° Viale Marconi. 5, I – 24044 Dalmine (BG), ITALY, Tel. +39-035-2052339; Fax. +39-035-562779

Main Text

Comparative finite-element model analysis of ascending aortic flow in bicuspid and tricuspid aortic valve.

Francesca Viscardi[§], MD, Christian Vergara°, PhD, Luca Antiga^, PhD, Sabrina Merelli^, Alessandro Veneziani*, PhD, Giovanni Puppini[§], MD, Giuseppe Faggian[§], MD, Alessandro Mazzucco[§], MD, Giovanni Battista Luciani[§], MD.

§Divisions of Cardiac Surgery and Radiology, University of Verona, Italy;

°Deparment of Information Technology and Mathematical Methods, University of Bergamo, Italy;

^Mario Negri Institute, Bergamo, Italy;

*Department of Mathematics and Computer Science, Emory University, Atlanta, GA, U. S. A.

Short Title: Finite-element model analysis of aortic flow.

Key Words: Bicuspid Aortic Valve; Ascending Aorta; Finite-element Model; Haemodynamics.

Correspondence to:

Giovanni Battista Luciani, MD

Division of Cardiac Surgery

University of Verona

O. C. M. Piazzale Stefani 1

Verona, 37126, Italy

E-mail: giovanni.luciani@univr.it

Text word count:

Figure count:

Read at the 5th International Conference on Pediatric Mechanical Support Systems and Pediatric Cardiopulmonary Perfusion, Dallas, TX, May 27-30, 2009.

Abstract.

Purpose: In bicuspid aortic valve (BAV) disease the role of genetic and haemodynamic factors influencing ascending aortic pathology is controversial. In order to test the effect of BAV geometry on ascending aortic flow, a Finite Element model analysis was undertaken.

Methods: A surface model of aortic root and ascending aorta was obtained from magnetic resonance images of patients with BAV and tricuspid aortic valve using the segmentation facilities of the image processing code Vascular Modeling Toolkit (developed at the Mario Negri Institute). Simplified and however reliable analytical models of bicuspid (antero-posterior, AP, and latero-lateral, LL, commissures) and tricuspid orifices were mathematically defined. Final models were turned into a volumetric mesh of linear tetrahedra for computational fluid dynamics simulations. Numerical simulations were performed with the Finite Element code *LifeV* (developed by the research centers MOX-Milan, INRIA-Paris, EPFL-Lausanne). Physiological inflow boundary conditions at inlet were imposed by means of a mathematically sound and well tested method based on the introduction of a Lagrange multiplier in the problem formulation. The flow velocity fields were assessed for four levels: aortic annulus, sinus of Valsalva, sinotubular junction, ascending aorta.

Results: Comparison of finite-element model analysis of bicuspid and tricuspid aortic valve shows different blood flow velocity pattern. The flow in the AP bicuspid shows an asymmetrical distribution of velocity field towards the convexity of the mid-ascending aorta returning symmetrical in distal ascending aorta. In the LL bicuspid a less pronounced asymmetry is noted at the sinus of Valsalva level. On the contrary, tricuspid flow is symmetrical in each aortic segment. Moreover, aortic flow in bicuspid model gains a maximum velocity at the systole of 5.5 m/s for AP and of 5.7 m/s for LL, while in the tricuspid maximum velocity is 2.6 m/s.

Conclusions: Comparison between models shows an asymmetrical and higher flow velocity in the bicuspid models, in particular in the AP configuration. The asymmetry is more pronounced at the aortic level known to be more exposed to aneurysm formation in bicuspid patients. This supports the hypothesis that haemodynamic factors may contribute to ascending aortic pathology in this

subset of patients.

Introduction.

Bicuspid aortic valve (BAV) is the most common form of congenital heart disease, affecting 0.5-2% of the population [1]. It includes different morphological phenotypes and predisposes to aortic valvar pathology (stenosis, regurgitation or both) and aortic aneurysms at different levels, even in children and young adults, irrespective to severity of valvar dysfunction [2]. The pathogenesis of aortic dilation in the presence of BAV is still controversial. Histopathologic changes as cystic medial necrosis of the proximal aortic wall causing abnormal aortic distensibility and stiffness were identified in patients with BAV, similarly to Marfan patients [3]. A genetic basis accounting for both valve and wall defects was thus postulated (BAV syndrome). However, unlike patients with Marfan syndrome, patients with BAV do not suffer from pulmonary artery dilatation, countering the idea of an inherited tissue weakness [1]. In addition, recent studies have shown that a variety of genotypes is associated with the BAV phenotype [4]. Another possible explanation for aortic aneurysms in BAV patients is a patho-physiological phenomenon due to increased wall stress caused by abnormal blood flow in the aortic root through a stenotic BAV. Nonetheless, aortic dilation is noted also in patients with a functionally normal or regurgitant valve. One hypothesis is that the abnormal opening of the BAV, even if not stenotic or only mildly stenotic, may cause increased hemodynamic wall stress leading to aneurysm formation [5].

In order to elucidate the role of aortic valve morphology (bicuspid versus tricuspid) and orientation (bicuspid with antero-posterior versus bicuspid with latero-lateral commissures) on patterns of ascending aortic flow dynamics, a computational model of the aortic root was constructed. This allows to investigate in a non-invasive and in a quantitative way blood flow through the aortic valve. In particular, the aims of this study were to: 1) Create computational models of arterial vessels, starting from geometrical data obtained by digitalized magnetic resonance imaging (MRI). 2) Perform numerical simulations in these geometries by the Finite Element method, which allows to obtain the velocity pattern of blood in ascending aorta and to evaluate the subsequent risk for aneurysm formation in a stated site. 3) Examine qualitative differences in aortic blood flow between tricuspid valvular orifice and bicuspid ones.

Methods.

Patients and Cardiac Imaging

Six healthy subjects (aged 16-65 years) with incidental trans-thoracic echocardiographic (TTE) finding of BAV and eight with finding of tricuspid aortic valve (TAV) underwent cardiac MRI. TTE was used to detect aortic valve anatomy and to exclude relevant (moderate or greater) valve insufficiency and relevant (peak gradient > 20 mmHg) aortic stenosis. Aortic valve morphology was examined in parasternal long and short-axis views. A BAV was diagnosed when 2 cusps were clearly identified in short-axis view. Antero-posterior (AP) BAV, hereafter named type 1 BAV, was defined by the presence of fusion of right and left coronary cusps, while latero-lateral (LL) BAV, hereafter named type 2 BAV, when right coronary and non-coronary cusps were fused. Left ventricular outflow tract measurements, including ascending aorta, were carried out in two-dimensional parasternal long-axis approach at four levels (annulus, sinuses of Valsalva, sinotubular junction and proximal ascending aorta), perpendicular to the axis of the aorta at each level. Peak aortic velocity and peak and mean aortic gradients were assessed using the continuous-wave Doppler tecnique from different imaging planes. Doppler imaging was applied to measure the deceleration slope and pressure half-time of the aortic regurgitant jet. Trans-thoracic echocardiogram was performed with 2.5-MHz ultrasound transducers (Hewlett-Packard Sonos 2500 system) and recorded on VHS videotape.

MR imaging was obtained *in vivo* by a 1.5 Tesla machine (Magnetom Simphony, Siemens Medical Systems, Erlagen, Germany). Spin-echo sequences for morphological definition were obtained from the cardiac base to the aortic arch. For a multiphase imaging of the aortic valve sequences K-space turbo gradient echo (TrueFisp) were used, acquired during a 12-second breath hold for each view with retrogated ECG triggering, set acquisition window 20% above the average R-R interval. The following parameters were used: TE=1.6 msec; flip angle=65°; slice thickness=6 mm; temporal resolution=48 msec; field of view=400 mm; acquisition matrix=256x256. From the short axis plane, left ventricle outflow-tract cine sequences were acquired and ascending aortic flow was evaluated through cine gradient-echo images, highlighting its relation with the geometry of the opening of aortic leaflets.

Construction of the meshes from MRI data

A surface model of the aortic root, ascending aorta, aortic arch and thoracic aorta was obtained from MRI images using the segmentation facilities of an image processing research code called Vascular Modeling Toolkit [6]. In particular, this tool allows to generate a surface representing the lumen boundary located at the steepest lumen intensity change. An analytical model of a bicuspid valve orifice was mathematically defined on a two-dimensional plane by the intersection of two circle functions of different radius (Fig. 1). This function was sampled on the surface representing the aortic root inlet, and used to open an orifice resembling a typical bicuspid valve with given parameters aortic valve area, aortic valve orientation, position of the valve inside aorta. This was done for type 1 and type 2 BAV configurations as well as for tricuspid valve model. In particular, the area of the root was of 4.6 cm^2, the area of the tricuspid valve was of 3.2 cm^2 (corresponding to $x=y=z=9.8$ *mm* in Fig. 1), whilst the area of the bicuspid valves was of 2.0 cm^2 (corresponding to $x=4$, $y=6$, $z=9.8$ *mm* in Fig. 1). The orientation of the two bicuspid valve configurations was set according to the respective commissures (Fig. 2), with relative angles equal to 65°.

The final models were turned into volumetric meshes of linear tetrahedra in order for computational fluid-dynamics simulations to be carried out (Fig.3). In all the three meshes we have about 110000 tetrahedra and 60000 degrees of freedom.

Numerical simulations

Numerical simulations were performed in these computational domains with the Finite Element code LifeV (a program developed at the research centers MOX – Politecnico di Milano, INRIA –

Paris, EPFL – Lausanne and recently developed also at the University of Bergamo and at the Emory University – see www.lifev.org). The blood was considered as Newtonian, homogeneous and incompressible, so that the Navier-Stokes equations for incompressible fluids have been used for the mathematical description [7]. The fluid viscosity was set equal to 0.035 Poise and the density equal to 1.0 g/cm^3. P1/P1 stabilized Finite Elements were used. We resorted to a parallel implementation of our Finite Element solver, exploiting an 8 processors architecture. The vessel wall was considered rigid (fixed). At the inlet, physiological inflow boundary conditions (Fig.4) taken from [8] were chosen as representative of the heart action. These data were imposed by the introduction of a Lagrange multiplier [9,10]. This non standard mathematical technique, implemented into LifeV avoids any bias introduced by choosing *a priori* the shape of the velocity profile at the inlet, as commonly done following other practictioner approaches. The implementation of such technique and the numerical simulations presented in this work have been performed at University of Bergamo.

Results.

The numerical results obtained by the Finite Element method concern the velocity and the pressure of the blood in the reconstructed geometries. In particular, velocity pattern at the systole was assessed at four different aortic levels: 1) aortic annulus, 2) sinotubular junction, 3) sinus of Valsalva and 4) mid-ascending aorta. In Fig 5a the velocity patterns of type 1 BAV configuration at levels 2 and 4 (that is at sinotubular junction and at mid-ascending aorta) are plotted. At all the levels the velocity at each point is proportional to the height of the plotted profile. The same velocity patterns are reported for the type 2 configuration (Fig. 5b) and for the tricuspid geometry (Fig. 5c).

In Fig. 6, the vectors of the velocity field at time t=0.216 are plotted on a longitudinal section. In these figures, in order to highlight the differences among the three flow patterns (type 1 and type 2

BAV, TAV), the same velocity range in the bar plot was maintained.

The velocity patterns of aortic flow in bicuspid models gain a peak velocity at the systole two-fold greater than in the tricuspid model (5.5 m/s for type 1 configuration, 5.7 m/s for type 2 configuration, 2.6 m/s in TAV). Furthermore, comparison between the two different bicuspid configurations (AP in Fig. 6a and LL in Fig. 6b) highlights that flow in type 1 configuration is characterized by greater asymmetry than in type 2. The latter seems to be associated with asymmetry at the sinus of Valsalva rather than the mid-ascending aorta (i.e. more prominent Eddy currents at the aortic root level).

Discussion.

Mathematical modeling has been widely used to predict arterial aneurysm formation, even at the ascending aortic level [11]. The application of computational modeling with Finite Element analysis to solve the clinical question of aortic aneurysm formation relative to BAV represents a novel approach, as to our knowledge no prior work on this exists in the literature.

As such, several methodological assumptions were necessary to define the “model”. Each one of these represents a potential limitation to the model (see Limitations, below). Because of these restrictions, the data generated by these preliminary models is this far only qualitative. Nonetheless some information is interestingly consistent with previously reported clinical findings. In fact, some authors have pointed out that BAV phenotype can be correlated with severity and localization of aortic aneurysm formation. Histopathologic studies on diseased ascending aortas by Russo et al. [12] state that type 1 BAV is associated with earlier aneurysm formation and worse aortic wall degeneration than type 2 BAV in surgical patients. Echocardiographic findings by Schaefer et al. [13] confirm that type 1 BAV is characterized by a higher abnormal aortic distensibility and stiffness than type 2, with larger aortic diameter at the sinuses of Valsalva and smaller aortic arch. Further work by Schaefer and associated [14] led to observation that type 1 BAV is associated with normal aortic shape but greater aortic dimensions, whilst type 2 with abnormal aortic shape, ascending aortic dilatation, and larger arch dimensions, possibly related to the majority of stenotic valves in type 2 group.

We found for type 1 BAV flow an asymmetrical distribution of velocity field towards the convexity of the mid-ascending aorta, returning symmetrical in distal ascending aorta. For the type 2 BAV the asymmetry is evident, but less pronounced with respect to the type 1 case, while flow turbulences and Eddy currents are more pronounced and jet velocity higher. It is likely that the orientation of the BAV openings with respect to the plane of aortic curvature results in different jet shapes and different distribution of wall stress on the aorta. In our model type 1 is oriented less symmetrically with respect to the plane of aortic curvature, which leads to a stronger jet oriented towards the outer wall of the ascending aorta. Different wall stress could lead to vascular remodeling and aneurysm formation as observed in BAV patients, not only associated with the severity and mechanism of valve dysfunction but mainly with valve orientation.

Discrepancies, if any, between clinical (echocardiographic) observations [12, 13, 14] and the present numerical results are to be ascribed to the fact that most clinical series include diseased (to a varying extent) valves, mostly regurgitant. In this work the aortic orifice was set at an area compatible with normal (i. e. non-stenotic) valve function. This choice was deliberately done to distinguish the influence of aortic valve geometry on aortic flow pattern, and ultimately, on asymmetrical stress on the entire ascending aorta. It is noteworthy that the few clinical series where morphological subtypes of BAV were correlated with aortic dimensions, in the absence of significant valve dysfunction (normally functioning BAV) failed to demonstrate any association [15]. Indeed, BAV has thus far been thought to cause dilatation only due to stenotic orifice. Some authors [5, 16] have found that in stenotic BAV patients the antero-lateral region of the ascending aorta is subject to greater hemodynamic stress (measured with Doppler flow velocity) than in stenotic TAV patients. The present study offers preliminary evidence that even normally functioning BAV (i. e. non-stenotic) may generate flow patterns and velocity identical to those seen in post-stenotic hemodynamics (and dilatation). Our preliminary conclusion is that there is something inherent with aortic flow modeled by a two-leaflet valve that is intrinsically different (thus pathological) from three-leaflet valve flow. Echocardiographic works pointing out that, irrespective to the functional status of the valve, BAV is usually associated with a predominant enlargement of mid-ascending aorta support these findings [15]. In fact in our study mid-ascending aortic level is the one with maximum flow velocity and more pronounced jet asymmetry, especially in type 1 BAV. In addition, non-stenotic BAV with different orientation (and here analyzed are the two comprising the vast majority of theoretically infinite configurations) produce different level, and thus morphological types, of aortic aneurysm.

The present work suggests that the methodology here applied allows to generate mathematical models for computational fluid dynamics starting from clinical data (echocardiography, MRI). In addition, such method may enable solution of specific clinical questions (i.e. does number and orientation of aortic valve leaflets generate different flow patterns and fluid dynamics?) by abstraction and, ultimately, allow to return to the clinical setting with predictive information.

Limitations of the study

There are a few notable limitations to this study. First of all, the vessel wall was considered fixed. This assumption is not realistic for the aorta, but, due to its simplicity, the model was chosen to give insightful preliminary results. The study of the compliant model, which is more complex from the computational point of view, is under further investigation.

Secondly, the orientation, shape and area of the valves have been chosen as representative of the three different anatomic types, based on echocardiographic findings recorded from individuals thought to be representative of that BAV phenotype, as previously done by others [13]. This was a simplification, because, as clinicians and surgeons know, each BAV patient carries a slightly different valvular anatomy and function and aortic dimension. Furthermore, surgical (and pathological) classifications are often at variance with echocardiographic ones [12, 13, 14, 16, 17].

Nevertheless, a simplification is needed for the application of the proposed model. Obviously, choice of different valvar parameters might alter the final results. However, since the aim of this work is to give preliminary results with a chosen methodology, we focused on the two more commonly reported BAV morphologies (antero-posterior, type 1, and latero-lateral, type 2) in most cardiological and surgical series. The analysis of computational domains with slightly different parameters of valve (such as area and orientation) is still ongoing and may corroborate these findings.

Finally, we point out that the results presented herein are purely qualitative, being our main purpose to illustrate the eventual impact of an integrated multidisciplinary approach with some preliminary results However, the proposed conjectures will need to be supported by quantitative results. For this reason, future work will be focused on the quantification of some fluid-dynamics quantity. For example, it will be possible to consider the differential shear aortic wall stress and energy levels in order to detect if there is any correlation between the velocity patterns and the aneurysm formation.

Conclusions.

Comparison between the three models shows an asymmetrical and higher flow velocity in the bicuspid models. The asymmetry is different between the two phenotypes: the type 1 shows a higher velocity jet at the aortic level known to be more exposed to aneurysm formation in bicuspid patients, while the type 2 shows higher turbulence at the sinuses of Valsalva level. These findings support the hypothesis that hemodynamic factors may contribute to ascending aortic pathology in patients with BAV. They might also support the thesis that attributes differences in aortic dimensions between BAV phenotypes to inhomogeneous distribution of shear forces due to different relation of leaflet orientation with ascending aortic geometry.

References.

1) Guntheroth WG. A critical review of the American College of Cardiology/American Heart Association practice guidelines on bicuspid aortic valve with dilated ascending aorta. Am J Cardiol. 2008; 102:107-110.

2) Gurvitz M, Chang RK, Drant S, Allada V. Frequency of aortic root dilation in children with a bicuspid aortic valve. Am J Cardiol 2004; 94:1337-1340.

3) Bonderman D, Gharehbaghi-Schnell E, Wollenek G, Maurer G, Baumgartner H, Lang IM. Mechanisms underlying aortic dilatation in congenital aortic valve malformation. Circulation. 1999; 99(16):2138-43.

4) Ellison JW, Yagubyan M, Majumdar R, et al. Evidence of genetic locus heterogeneity for familial bicuspid aortic valve. J Surg Res. 2007; 142(1):28-31.

5) Bauer M, Siniawski H, Pasic M, Schaumann B, Hetzer R. Different hemodynamic stress of the ascending aorta wall in patients with bicuspid and tricuspid aortic valve. J Card Surg. 2006; 21(3):218-20.

6) Antiga L, Piccinelli M, Botti L, Ene-Iordache B, Remuzzi A, Steinman DA. An image-based modeling framework for patient-specific computational hemodynamics. Med Biol Eng Comput. 2008 Nov; 46(11):1097-112.

7) Chorin AJ, Marsden JE. A mathematical introduction to fluid mechanics. 3rd Edition. Springer (2000).

8) Avolio AP. Multi-branched model of the human arterial system. Med Biol Eng Comp. 1980; 18: 709-718.

9) Formaggia L, Gerbeau JF, Nobile F, Quarteroni A. Numerical treatment of defective boundary conditions for the Navier-Stokes equation. SIAM J Num Anal. 2002; 40-1:376-401.

10) Veneziani A, Vergara C. Flow rate defective boundary conditions in haemodinamics simulations. Int J Num Meth Fluids. 2005; 47:803-816.

11) Poullis MP, Warwick R, Oo A, Poole RJ. Ascending aortic curvature as an independent risk factor for type A dissection, and ascending aortic aneurysm formation: a mathematical model. Eur J Cardiothorac Surg. 2008; 33(6): 995-1001.

12) Russo CF, Cannata A, Lanfranconi M, Vitali E, Garatti A, Bonacina E. Is aortic wall degeneration related to bicuspid aortic valve anatomy in patients with valvular disease?. J Thorac Cardiovasc Surg. 2008; 136(4):937-42

13) Schaefer BM, Lewin MB, Stout KK, Byers PH, Otto CM. Usefulness of bicuspid aortic valve phenotype to predict elastic properties of the ascending aorta. Am J Cardiol. 2007; 99(5):686-90

14) Schaefer BM, Lewin MB, Stout KK, et al. The bicuspid aortic valve: an integrated phenotypic classification of leaflet morphology and aortic root shape. Heart. 2008; 94(12):1634-8

15) Cecconi M, Manfrin M, Moraca A, et al. Aortic dimensions in patients with bicuspid aortic valve without significant valve dysfunction. Am J Cardiol. 2005; 95(2):292-4.

16) Della Corte A, Romano G, Tizzano F, Amarelli C, et al. Echocardiographic anatomy of ascending aorta dilatation: correlations with aortic valve morphology and function. Int J Cardiol. 2006; 113(3):320-6.

17) Sievers HH, Schmidtke C. A classification system for the bicuspid aortic valve from 304 surgical specimens. J Thorac Cardiovasc Surg. 2007;133(5):1226-33.

Legends to Figures.

Figure 1.

Intersection of two circle functions of different radius in order to determine the different valves. Tricuspid valve correspond to *x=y=z=9.8 mm,* bicuspid ones to *x=4, y=6, z=9.8*.

Figure 2.

Schematic classification of BAV phenotypes with respect to TAV in an orientation similar to echocardiographic parasternal short-axis view: A, type 1 BAV (fusion of left and right coronary cusps); B, type 2 BAV (fusion of right coronary and non-coronary cusps); C, TAV.

Figure 3.

Mesh representing ascending aorta. The three valve orifice models are also presented: A, type 1 BAV; B, type 2 BAV; C, TAV.

Figure 4.

Flow rate boundary condition prescribed at the inlet of the ascending aorta as representative of the heart action (taken from [8]).

Figure 5.

Velocity patterns at systole in ascending aorta at levels: sinus of Valsalva (2) and mid-ascending aorta (4). At all the levels the velocity at each point is proportional to the height of the plotted profile. The three valve models are presented: A, type 1 BAV; B, type 2 BAV; C, TAV. The asymmetry of the velocity pattern at the sinus of Valsalva is evident for bicuspid valves (in particular for type 1 BAV).

Figure 6.

Vectors of velocity field plotted in a longitudinal section. On each of the selected points, a vector with length proportional to the magnitude of the velocity field and with the same direction of the field, is plotted. The three valve models are presented: A, Type 1 BAV; B, Type 2 BAV; C, TAV. Again, the asymmetry of the flow in the bicuspid valves, in particular for type 1 BAV, is pointed out.

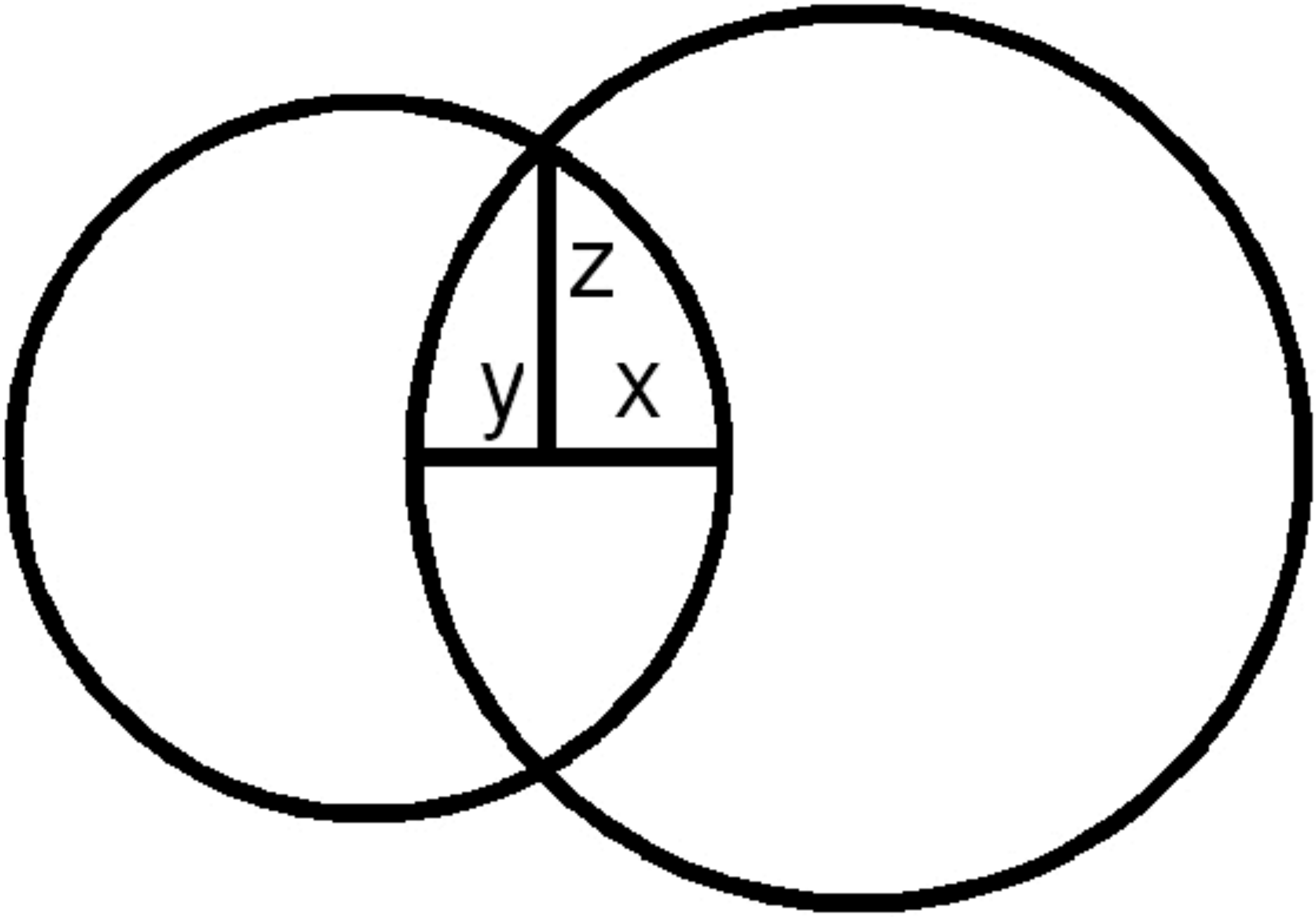
z
y
x

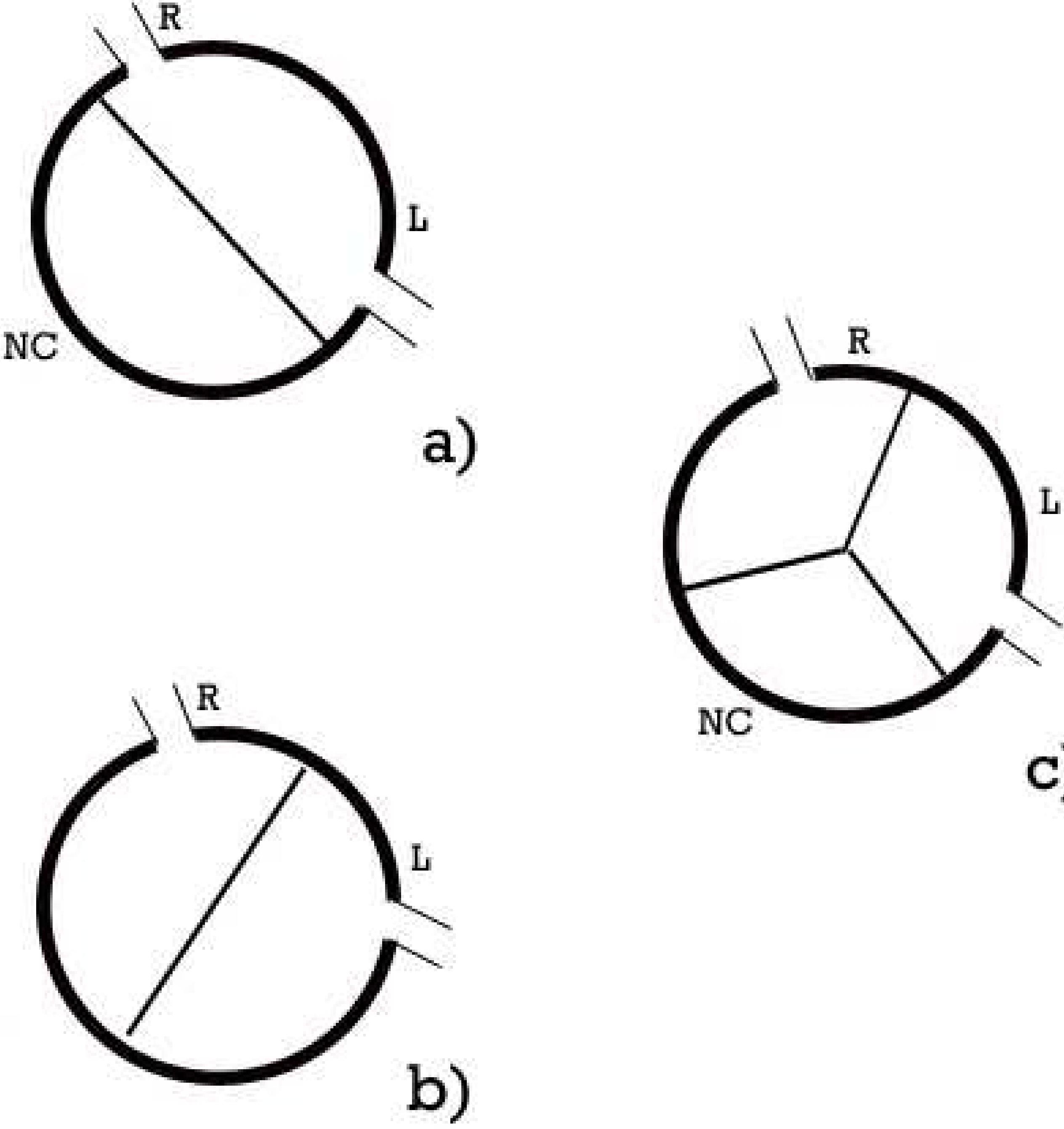
R
L
NC
a)
R
L
NC
c)
R
L
b)

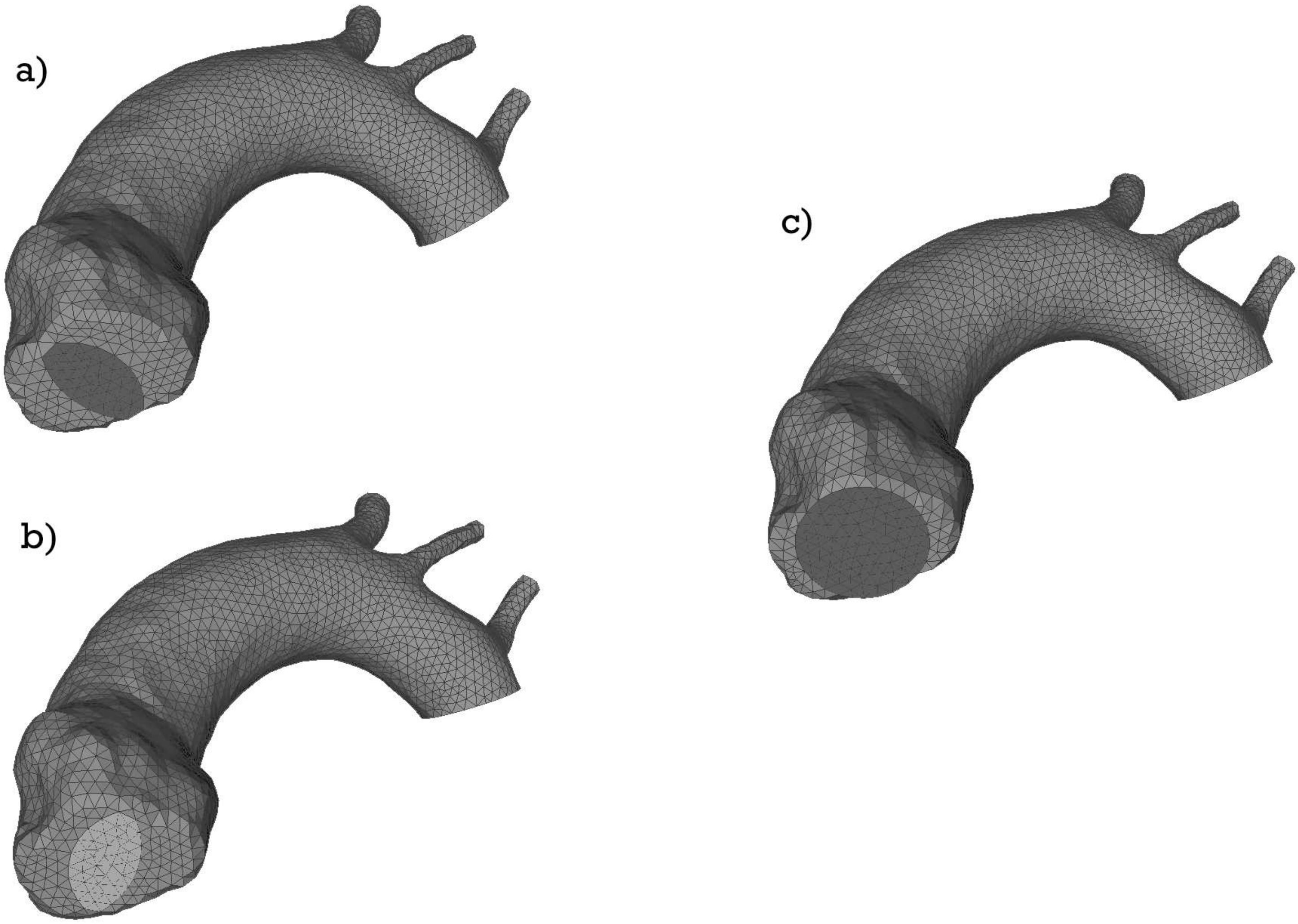
a)
b)
c)

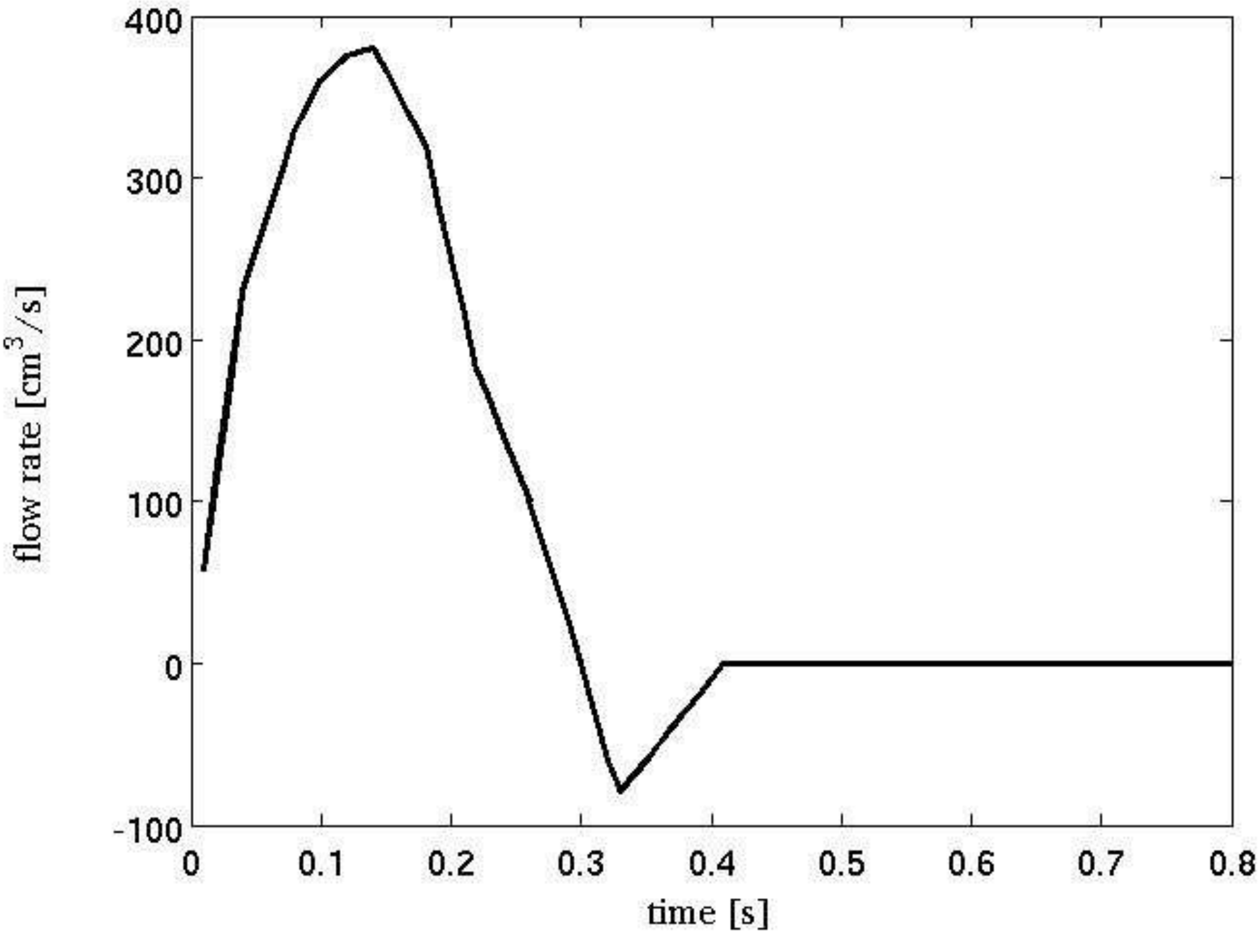
400
300
200
100
0
-100
0
0.1
0.2
0.3
0.4
0.5
0.6
0.7
0.8
flow rate [cm^3/s]
time [s]

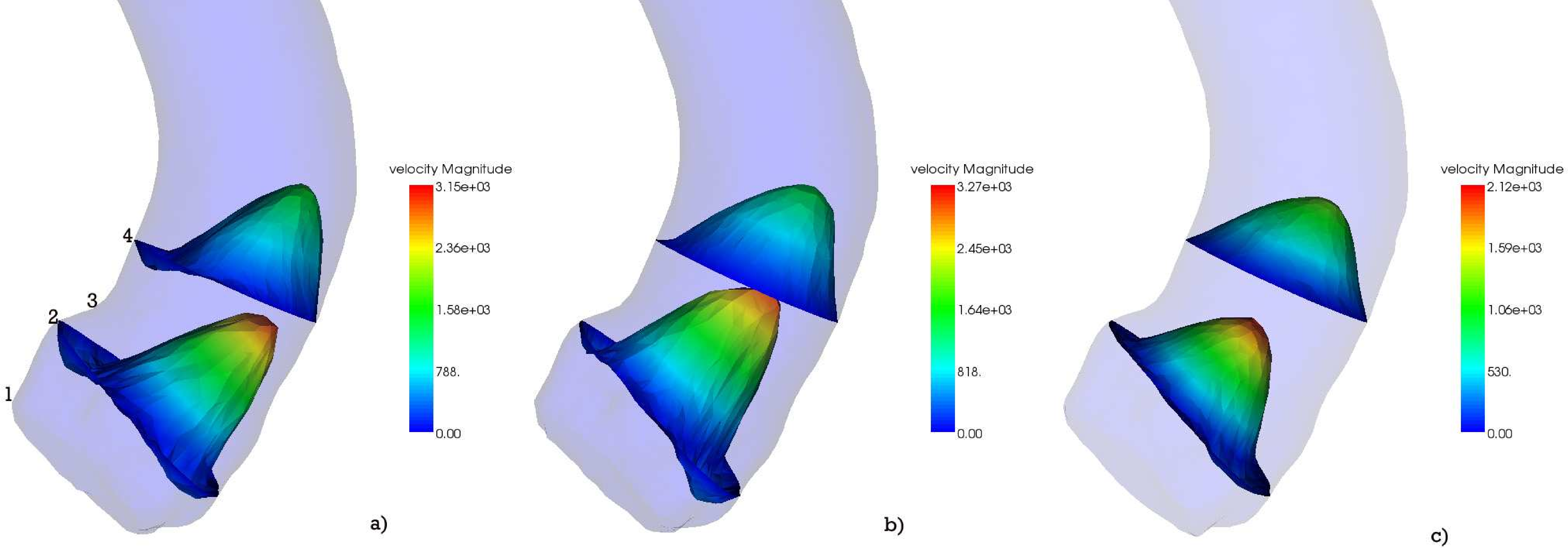

1
2
3
4
velocity Magnitude
3.15e+03
2.36e+03
1.58e+03
788.
0.00
a)
velocity Magnitude
3.27e+03
2.45e+03
1.64e+03
818.
0.00
b)
velocity Magnitude
2.12e+03
1.59e+03
1.06e+03
530.
0.00
c)

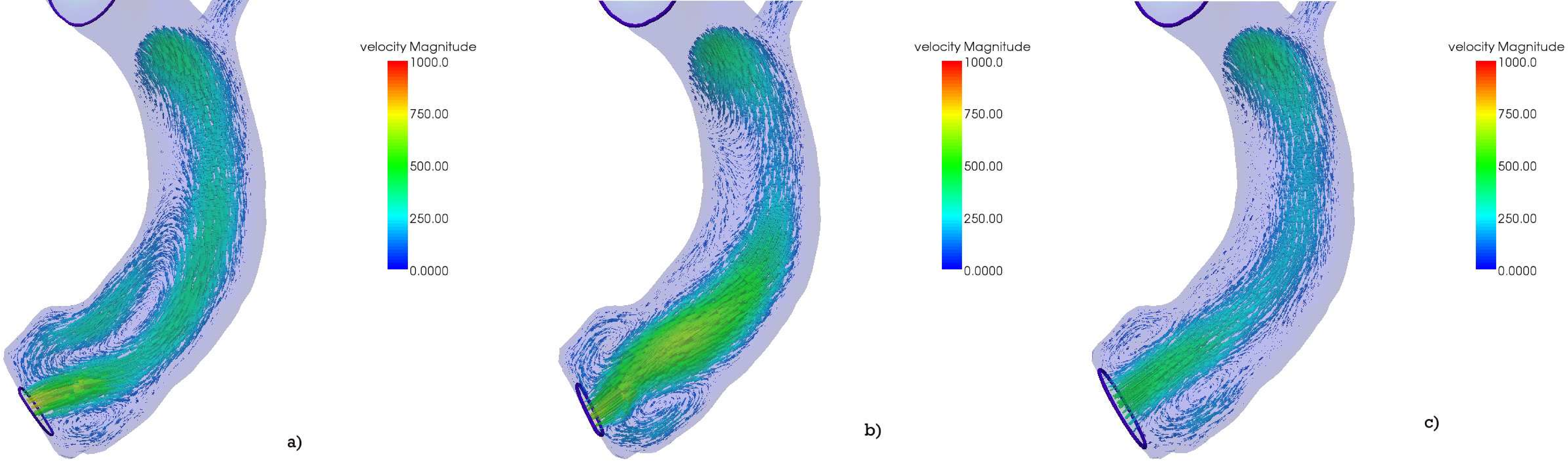
velocity Magnitude
1000.0
750.00
500.00
250.00
0.0000
a)
velocity Magnitude
1000.0
750.00
500.00
250.00
0.0000
b)
velocity Magnitude
1000.0
750.00
500.00
250.00
0.0000
c)